Delineation of spatial tissue signatures of immunotherapy response groups in non-small cell lung cancer (NSCLC) - 118

Arutha Kulasinghe[1*], James Monkman[1], Honesty Kim[2], Aaron Mayer[2], Ahmed Mehdi[3], Nicolas Matigian[3], Marie Cumberbatch[4], Milan Bhagat[4], Dan Winkowski[5], Fabian Schneider[5], Jeppe Thaagard[5], James Mansfield[5], Rahul Ladwa[6], Scott N Muller[7], Mark Adams[8], Ken O'Byrne[8] *[1] University of Queensland Diamantina Institute, The University of Queensland, Brisbane, QLD, **Australia**. [2] Enable Medicine, Menlo Park, CA, USA. [3] Qfab Bioinformatics, The University of Queensland, Brisbane, QLD, Australia. [4] Tristar Technologies Group, Rockville, MD, USA. [5] Visiopharm, Denmark., [6]Princess Alexandra Hospital, Brisbane, QLD, Australia. [7] The University of Melbourne, Vic, Australia. [8] Queensland University of Technology, Brisbane, QLD, Australia. ***Corresponding author: arutha.kulasinghe@uq.edu.au @aruthak***

Immunotherapies, such as immune checkpoint inhibitors (ICI) have shown durable benefit in a subset of non-small cell lung cancer (NSCLC) patients. The mechanisms for this are not fully understood, however the composition and activation status of the cellular milieu contained within the tumour microenvironment (TME) is becomingly increasingly recognised as a driving factor in treatment-refractory disease.

Here, we employed multiplex IHC (mIHC), and Nanostring GeoMx digital spatial profiling (DSP) to capture the targeted immune proteome (60-plex) and transcriptome (1800-plex) of tumour and TME compartments, from a tissue microarray (TMA) of pre-treatment samples from a 2nd line NSCLC ICI-treated cohort (n=41 patients; n=25 responders, n=16 non-responders) in collaboration with Tristar Technologies.

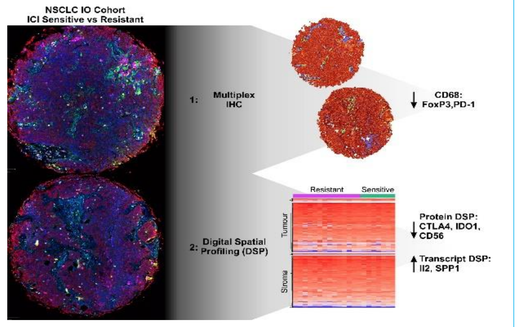

Methods

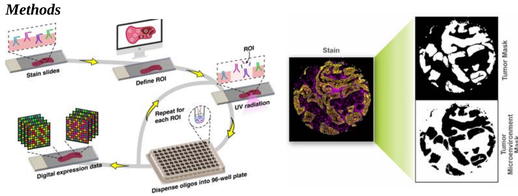

Digital spatial profiling of lung TMA cores as described in Sadegirad et al., CTI 2020. A strategy of masking for 'cytokeratin' and 'non-cytokeratin' was used to capture the 'tumour' and 'stromal' regions per core, respectively.

Patient Clinicopathological findings.

IO Cohort	Non-responder, N = 25	Responder, N = 16
Gender		
F	9 (36%)	5 (31%)
M	16 (64%)	11 (69%)
Age	66 (59, 69)	58 (58, 63)
ICI Treatment		
Durvalumab	0 (0%)	1 (6.2%)
Nivolumab	22 (88%)	11 (69%)
Pembrolizumab	3 (12%)	4 (25%)
Current Status		
Alive	8 (32%)	15 (94%)
Deceased	17 (68%)	1 (6.2%)
Histology		
Adenocarcinoma	12 (48%)	13 (81%)
Squamous Cell Carcinoma	13 (52%)	3 (19%)

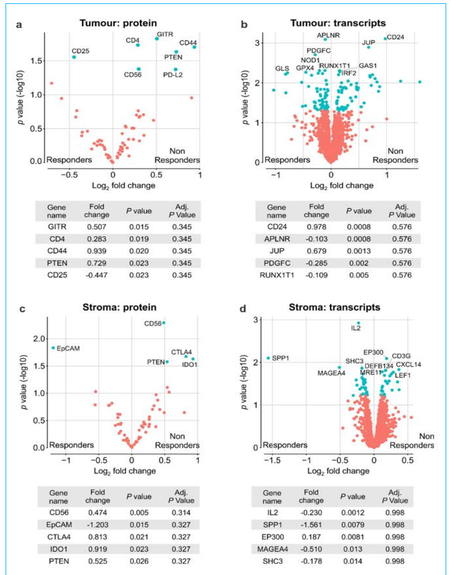

Gene name	Fold change	*P* value	Adj. *P* Value
GITR	0.507	0.015	0.345
CD4	0.283	0.019	0.345
CD44	0.939	0.020	0.345
PTEN	0.729	0.023	0.345
CD25	-0.447	0.023	0.345

Gene name	Fold change	*P* value	Adj. *P* Value
CD24	0.978	0.0008	0.576
APLNR	-0.103	0.0008	0.576
JUP	0.679	0.0013	0.576
PDGFC	-0.285	0.002	0.576
RUNX1T1	-0.109	0.005	0.576

Gene name	Fold change	*P* value	Adj. *P* Value
CD56	0.474	0.005	0.314
EpCAM	-1.203	0.015	0.327
CTLA4	0.813	0.021	0.327
IDO1	0.919	0.023	0.327
PTEN	0.525	0.026	0.327

Gene name	Fold change	*P* value	Adj. *P* Value
IL2	-0.230	0.0012	0.998
SPP1	-1.561	0.0079	0.998
EP300	0.187	0.0081	0.998
MAGEA4	-0.510	0.013	0.998
SHC3	-0.178	0.014	0.998

Figure 1. Volcano plots of differentially expressed proteins and RNA enriched for in the response/non-response groups in the tumour (A, B) and stroma (C,D) compartments. Significant DEG in blue.

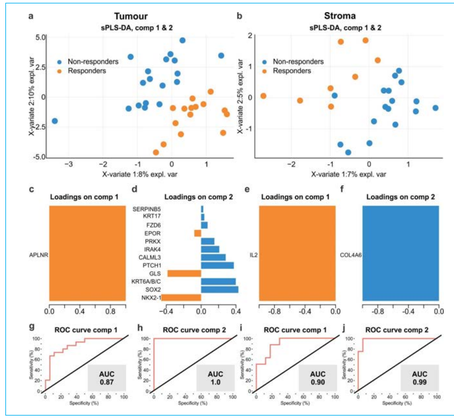

Figure 2. Multivariate sPLS-DA of mRNA features that distinguish NSCLC IO response. Patient sample discrimination defined by components 1 and 2 of sPLS-DA model for tumour (A) and stroma (B). (C) Component 1 loading for tumour regions. (D) Component 2 loading for tumour regions. (E) Component 1 loading for stroma. (F) Component 2 loading for stroma. (G) ROC curve to evaluate component 1 tumour signature. (H) ROC curve to evaluate component 2 tumour signature. (I) ROC curve to evaluate component 1 stroma signature. (J) ROC curve to evaluate component 2 stroma signature. Colour of component loadings indicates patient group in which feature was maximally expressed. Positive or negative values in bar chart indicate positive or negative contribution to the discriminant signature. Blue = Non-responder, Orange = Responder.

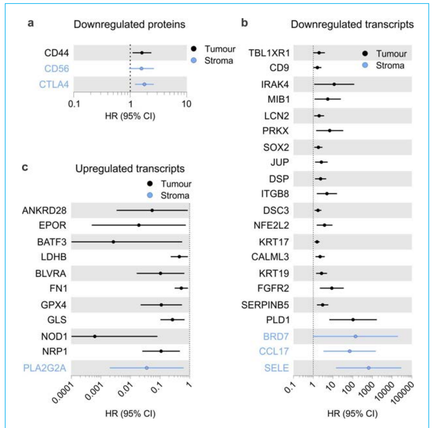

Figure 3. Cox proportional hazard survival analysis of differentially expressed protein and mRNA features by ICI response. (A) Forest plot showing HR and 95% CI of downregulated proteins. (B) Forest plot showing HR and 95% CI of downregulated transcripts. (C) Forest plot showing HR and 95% CI of upregulated transcripts

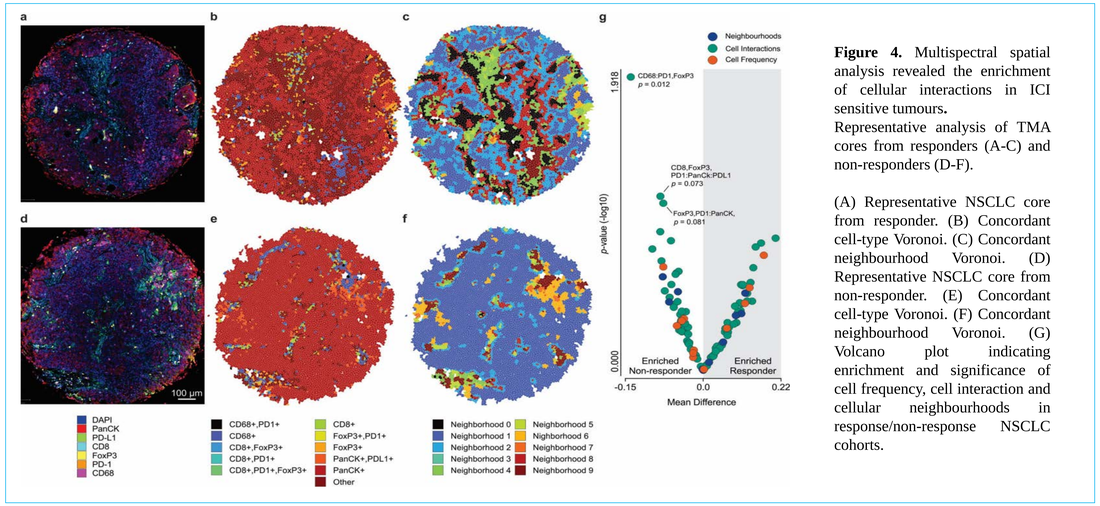

Figure 4. Multispectral spatial analysis revealed the enrichment of cellular interactions in ICI sensitive tumours**.**
Representative analysis of TMA cores from responders (A-C) and non-responders (D-F).

(A) Representative NSCLC core from responder. (B) Concordant cell-type Voronoi. (C) Concordant neighbourhood Voronoi. (D) Representative NSCLC core from non-responder. (E) Concordant cell-type Voronoi. (F) Concordant neighbourhood Voronoi. (G) Volcano plot indicating enrichment and significance of cell frequency, cell interaction and cellular neighbourhoods in response/non-response NSCLC cohorts.

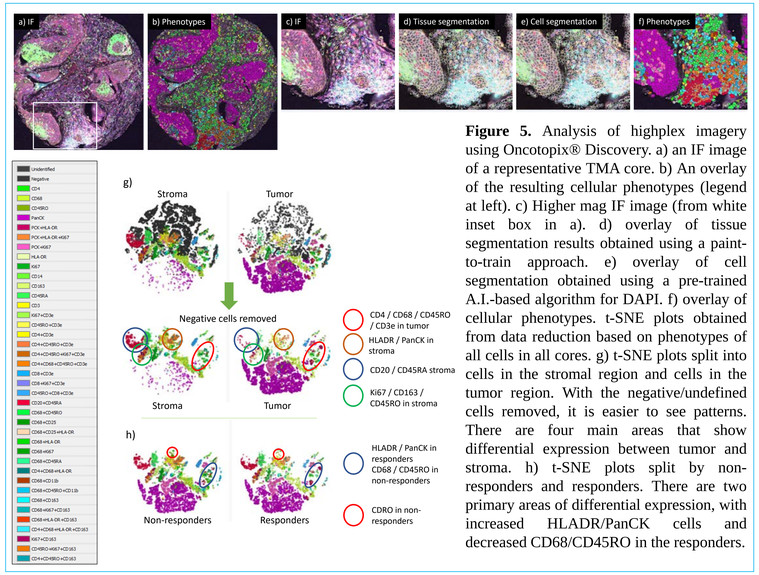

Figure 5. Analysis of highplex imagery using Oncotopix® Discovery. a) an IF image of a representative TMA core. b) An overlay of the resulting cellular phenotypes (legend at left). c) Higher mag IF image (from white inset box in a). d) overlay of tissue segmentation results obtained using a paint-to-train approach. e) overlay of cell segmentation obtained using a pre-trained A.I.-based algorithm for DAPI. f) overlay of cellular phenotypes. t-SNE plots obtained from data reduction based on phenotypes of all cells in all cores. g) t-SNE plots split into cells in the stromal region and cells in the tumor region. With the negative/undefined cells removed, it is easier to see patterns. There are four main areas that show differential expression between tumor and stroma. h) t-SNE plots split by non-responders and responders. There are two primary areas of differential expression, with increased HLADR/PanCK cells and decreased CD68/CD45RO in the responders.

Conclusion

Through multi-modal approaches, we have dissected the characteristics of NSCLC treatment groups and provide evidence for the role of several markers including IL2, CD25, CD44 and SPP1 in the efficacy of current generations of ICI therapy. Whilst further validation of putative markers is needed, our findings provide early insights into predictive biomarkers associated with response to therapy in NSCLC.